

mutations described here are probably the result of reduced or abolished function of the *pha-1* gene. In order to identify the phenotype presented by complete absence of *pha-1* (null phenotype), we isolated a deficiency, *tDf2*, which fails to complement not only *pha-1* but also both flanking genes, *vab-7* and *tra-1* (Fig. 3), and therefore has most likely completely lost the *pha-1* locus. The phenotype of homozygous *tDf2* embryos is very similar to that of the strong *pha-1* alleles (Table 1). Thus, complete removal of *pha-1* function results in defective pharynx differentiation. Another deficiency, *eDf20* (formerly *e1855*) (6), also fails to complement *pha-1* and *tra-1*. Its phenotype is similar to that of weak *pha-1* alleles, suggesting that some *pha-1* function is still present.

Animals homozygous for the temperature-sensitive *pha-1* alleles *e2123* and *t1001* grow to fertile, wild-type-looking hermaphrodites and males of wild-type morphology when shifted to nonpermissive temperature (25°C) after embryogenesis and hatching at permissive temperature (15°C). Temperature-shift experiments during embryogenesis show that the temperature-sensitive phases of both temperature-sensitive alleles begin during the proliferation phase and end at the 1½-fold stage of embryogenesis (Fig. 4).

The defect in pharynx development observed in *pha-1* mutants indicates that there are at least two steps in embryonic pharynx development. Early pharynx development does not require *pha-1* function since, in mutant embryos, pharyngeal cells are generated, a basement membrane is formed, and an early muscle cell-specific antigen is expressed. Later pharynx development, however, requires *pha-1* function, as expression of later markers in three of five pharyngeal cell types and morphogenesis of the pharynx are blocked in mutant embryos. Thus, cells that have already acquired their identities do not continue to differentiate but require an additional cue. The temperature-shift experiments indicate that *pha-1* only functions during embryogenesis and is not required for the continued expression of pharynx components such as myosin during postembryonic growth. Therefore, *pha-1* appears to be a gene involved in the control of the latter stages of differentiation and morphogenesis of the pharynx.

The identification of an organ-specific gene provides further evidence against the original thought that the *C. elegans* body is largely put together in a piecemeal manner by cell-autonomously determined cell lineages (2, 5). To our knowledge, organ-specific lack of differentiation has rarely been observed. The other examples of organ-specific genes that have been described are

cardiac lethal (7) and *eyeless* (8) in the Mexican axolotl and may be involved in inductive interactions, as shown by transplantation experiments. The gene *pha-1* may similarly be involved in an inductive interaction. Alternatively, *pha-1* could be required autonomously in all pharynx cells—for example, to turn on expression of late differentiation functions in the pharynx of *C. elegans*.

REFERENCES AND NOTES

1. C. Nüsslein-Volhard and E. Wieschaus, *Nature* **287**, 795 (1980).
2. J. E. Sulston, E. Schierenberg, J. G. White, J. N. Thomson, *Dev. Biol.* **100**, 64 (1983).
3. All developmental times refer to time after the first cleavage at 20°C, unless otherwise indicated.
4. D. G. Albertson and J. N. Thomson, *Philos. Trans. R. Soc. London Ser. B* **275**, 299 (1976).
5. J. R. Priess and J. N. Thomson, *Cell* **48**, 241 (1987).
6. J. Hodgkin, *Genes Dev.* **1**, 731 (1987).
7. R. R. Humphrey, *Dev. Biol.* **27**, 365 (1972).
8. L. G. Epp, *Am. Zool.* **18**, 267 (1978).
9. A mutation in *pha-1*, *e2123*, was isolated from a screen of 22,000 F2 progeny of mutagenized, wild-type, strain Bristol *C. elegans* for animals that produced viable progeny at 15°C, but nonviable eggs at 25°C. By Nomarski light microscopic observation of terminal stage embryos, *pha-1(e2123)* was identified as a mutation resulting in an undifferentiated pharynx. Further alleles of *pha-1(t1001, e2275, e2286, and*

t1002) were isolated from crosses of mutagenized wild-type or *tra-1(e1099)* males with hermaphrodites of genotype *pha-1(e2123) dpy-18(e499) III*, or *bli-3(e767) cib-1(e2300) I; vab-7(e1562) pha-1(e2123) III*. A total of 25,200 F1 cross progeny were tested for temperature-sensitive embryonic lethality. Allele *pha-1(e2468)* was isolated in an independent screen for embryonic lethal mutations (J. H. Rothman, personal communication). Deficiency *eDf20* was obtained (6).

10. J. Sulston and J. Hodgkin, in *The Nematode Caenorhabditis elegans*, W. B. Wood, Ed. (Cold Spring Harbor Laboratory, Cold Spring Harbor, NY, 1988), pp. 587–606.
11. H. Okamoto and J. N. Thomson, *J. Neurosci.* **5**, 643 (1985).
12. H. F. Epstein, D. M. Miller III, L. A. Gossett, R. M. Hecht, in *Muscle Development*, M. Pearson and H. Epstein, Eds. (Cold Spring Harbor Laboratory, Cold Spring Harbor, NY, 1982), pp. 7–14.
13. S. Strome and W. B. Wood, *Proc. Natl. Acad. Sci. U.S.A.* **79**, 1558 (1982).
14. R. M. Pruss et al., *Cell* **27**, 419 (1981).
15. D. Albertson, *Dev. Biol.* **101**, 61 (1984).
16. Map data were submitted to the Caenorhabditis Genetics Center.
17. Part of this work was supported by Otto Hahn fellowships of the Max-Planck-Gesellschaft and by EMBO fellowships. We thank F. Bonhoeffer, C. Nüsslein-Volhard, and the Deutsche Forschungsgemeinschaft for support of our work and T. Bogaert, W. Driever, and J. Sulston for comments on the manuscript. Some strains were provided by the Caenorhabditis Genetic Center.

22 March 1990; accepted 11 July 1990

Changes in Sodium Channel Gating Produced by Point Mutations in a Cytoplasmic Linker

J. RANDALL MOORMAN,* GLENN E. KIRSCH, ARTHUR M. BROWN, ROLF H. JOHO

Voltage-gated sodium channels are transmembrane proteins of approximately 2000 amino acids and consist of four homologous domains (I through IV). In current topographical models, domains III and IV are linked by a highly conserved cytoplasmic sequence of amino acids. Disruptions of the III-IV linker by cleavage or antibody binding slow inactivation, the depolarization-induced closed state characteristic of sodium channels. This linker might be the positively charged "ball" that is thought to cause inactivation by occluding the open channel. Therefore, groups of two or three contiguous lysines were neutralized or a glutamate was substituted for an arginine in the III-IV linker of type III rat brain sodium channels. In all cases, inactivation occurred more rapidly rather than more slowly, contrary to predictions. Furthermore, activation was delayed in the arginine to glutamate mutation. Hence, the III-IV linker does not simply act as a charged blocker of the channel but instead influences all aspects of sodium channel gating.

THE AMINO ACID SEQUENCES OF many voltage-gated ion channels have been identified, and segments responsible for channel gating and ion conduction have been proposed. A highly con-

served segment links domains III and IV of the voltage-dependent Na⁺ channel (1–3) (Fig. 1A). This linker has a role in Na⁺ channel gating, since antibodies against a peptide sequence within this region delay Na⁺ current inactivation in skeletal myoballs when applied from the cytoplasmic surface (4), and coinjection of mRNAs encoding domains I to III with mRNAs encoding only domain IV of the type II Na⁺ channel produces slowly inactivating Na⁺ currents in *Xenopus* oocytes (5). A physical basis for these findings was originally sug-

J. R. Moorman, Department of Medicine, University of Texas Medical Branch, Galveston, TX 77550.
G. E. Kirsch, A. M. Brown, R. H. Joho, Department of Molecular Physiology and Biophysics, Baylor College of Medicine, Houston, TX 77030.

*To whom correspondence should be addressed at the Department of Internal Medicine, University of Virginia Health Sciences Center, Charlottesville, VA 22908.

gested on the basis of the observation that endopeptidases removed Na⁺ current inactivation without affecting activation (6). This was the "ball and chain" model for Na⁺

channel inactivation gating in which a positively charged cytoplasmic ball is attracted electrostatically to a negatively charged site in the channel that is exposed after the

activation gate has opened. The III-IV linker has subsequently been proposed by numerous groups (1, 2, 5, 7) to act as the positively charged ball. We tested this hypothesis by making point mutations of positively charged residues in the III-IV linker of the rat brain type III Na⁺ channel and measuring Na⁺ currents expressed in mRNA-injected *Xenopus* oocytes (8). Contrary to expectations, conversion of two or three lysines to asparagines produced faster rather than slower inactivation of Na⁺ currents. Also unexpected was that the effects of removing positive charge were not limited to inactivation; conversion of the sole arginine in the linker to glutamate delayed activation.

Families of whole oocyte Na⁺ currents are shown in Fig. 1. These currents, which were blocked by tetrodotoxin (100 nM) and absent in uninjected oocytes, represent expression of type III (Fig. 1B) or mutated (Fig. 1, C to E) type III Na⁺ channel mRNAs. Our strategy was to replace contiguous lysines with asparagines, neutralizing the positive charges. In mutation M1 we replaced lysines 1426 to 1428 with asparagines; the resulting mRNA did not express measurable Na⁺ current. For mutation M2 we replaced lysines 1441 and 1442, and for mutation M4 we replaced lysines 1453, 1454, and 1457 with asparagines. Each of these five lysines except the lysine at 1457 is included in the peptide used to generate the antibodies that blocked inactivation (4). For mutation M5 we replaced the arginine (1461) with glutamate, producing the same net change in charge (-2) as in mutation M2.

The whole oocyte voltage-clamp records show that Na⁺ currents expressed after injection of M2 or M4 mRNAs decayed more rapidly. This was observed at all potentials (Fig. 1F). Current decay was described by a sum of two exponentials, and we compared the value of the faster time constant (τ) as a function of test potential for type III and M4 currents (Fig. 1G). Not only were the values of these faster time constants smaller in the M4 currents, but the faster component was also more heavily weighted at all test potentials in the M4 currents. These findings were reproducible with mRNAs from two transcription reactions injected into at least 20 oocytes from at least five frogs. The current-voltage relation expressed by type III and the M2, M4, and M5 mutated type III mRNAs were similar (9), with the largest currents evoked by depolarizations between -5 and 5 mV. Hence, shifts in the voltage dependence of gating are unlikely to be responsible for the increased rates of inactivation.

The two-microelectrode voltage clamp has a low frequency response (10) and can-

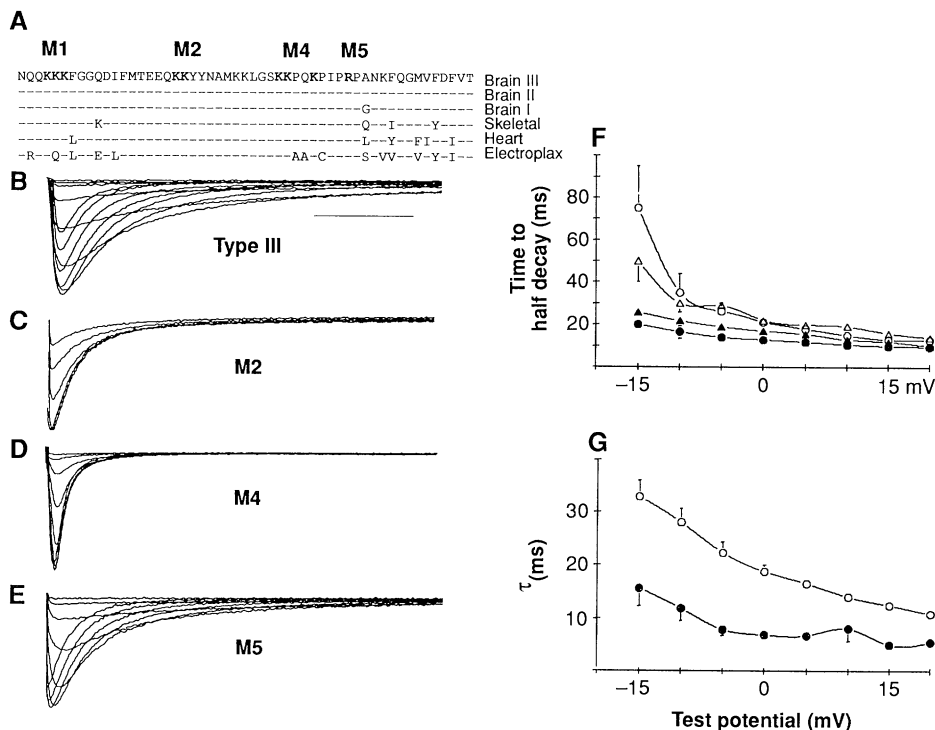
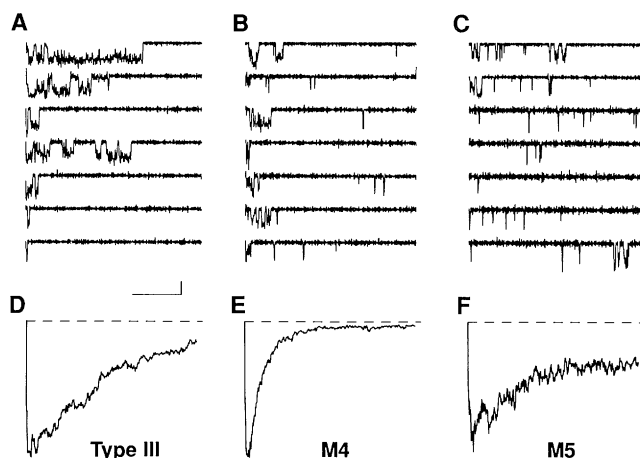


Fig. 1. (A) Amino acid sequences of the regions linking domains III and IV of Na⁺ channels. Amino acids 1423 to 1475 of the type III Na⁺ channel are aligned with the corresponding regions of other known Na⁺ channels. Positions of mutations are indicated in boldface. Lysine residues were changed to asparagines, and the arginine at 1461 was replaced by a glutamate. Abbreviations for the amino acid residues are A, Ala; C, Cys; D, Asp; E, Glu; F, Phe; G, Gly; H, His; I, Ile; K, Lys; L, Leu; M, Met; N, Asn; P, Pro; Q, Gln; R, Arg; S, Ser; T, Thr; V, Val; W, Trp; and Y, Tyr. (B) Type III currents. (C) M2 currents. (D) M4 currents. (E) M5 currents. (B to E) Families of whole oocyte currents elicited by depolarizing voltage steps from a holding potential of -90 mV to a test potential of -20 mV and in 5-mV increments thereafter in oocytes injected with type III Na⁺ channel mRNAs. Capacitative and leak components of the currents were corrected by subtracting current records in the presence of 100 nM tetrodotoxin. Bar, 50 ms; approximate peak current amplitudes are (B) 1250 nA, (C) 500 nA, (D) 600 nA, and (E) 500 nA. (F and G) Voltage dependence of current decay. (F) The time to 50% decay of the whole oocyte currents is plotted as a function of test potential for type III Na⁺ currents and the three mutations. Data points are the mean \pm SD for five or six oocytes from at least two frogs. \circ , Type III; \blacktriangle , mutation M2; \bullet , mutation M4; and \triangle , mutation M5. (G) The fast time constant of current decay (τ) for type III and M4 currents is plotted as a function of test potential. This time constant was more heavily weighted for the currents through the mutant channels (for example, $98 \pm 2\%$ in the mutant versus $85 \pm 3\%$ at test potential 0 mV, mean \pm SD, $n = 6$ oocytes each). \circ , Type III; and \bullet , mutation M4.

Fig. 2. Consecutive single-channel records (A to C) and ensemble average currents (D to F) at a test potential of 0 mV from cell-attached patches of oocytes injected with type III, M4, and M5 mRNA. Bar, 25 ms and 0.5 pA (single-channel recordings). The ensemble averages were constructed by pooling normalized average currents from cell-attached patches containing expressed type III (5 patches, 609 traces, 24 nulls, 3414 openings), M4 (5 patches, 651 traces, 55 nulls, 2639 openings), and M5 (5 patches, 600 traces, 202 nulls, 2145 openings) channels.



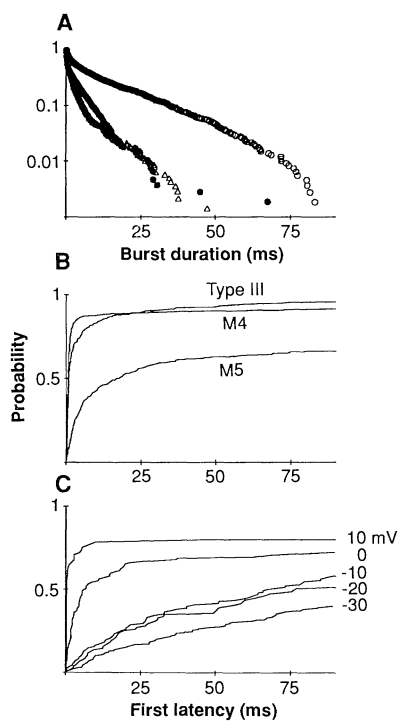


Fig. 3. Kinetic analysis at room temperature and a test potential of 0 mV of pooled data. The data set is the same as in Fig. 2. **(A)** Burst duration probability distribution for (○) type III, (●) M4, and (△) M5 channels. Closed time distributions were biexponential (not shown), and a critical closed time (12) was used to identify bursts of openings. The critical closed times were similar for all kinds of channels (2.4 to 2.8 ms). **(B)** Waiting time to first opening cumulative distributions. Data from multiple patches were corrected for the apparent number of channels, estimated from the number of overlapping events at test potential 0 mV, and the results pooled. **(C)** Voltage dependence of activation gating in a patch with a single M5 channel. This patch was one of five used in the pooled data (A and B).

not be used for detailed kinetic analysis. Therefore, we analyzed the mutants with patch-clamp recording of single-channel currents. Single-channel Na⁺ currents from type III, M4, and M5 channels at a test potential of 0 mV are shown in Fig. 2. Mutation M2 was not expressed well, so we did not measure single-channel currents for this mutant. Type III channels have two distinct patterns of gating, one characterized by brief openings at the beginning of voltage steps (fast gating) and the other by bursts of long openings (slow gating) (11). Mutations M4 and M5 showed a more uniform pattern of short bursts (Fig. 2, B and C). Ensemble averages of single-channel records pooled from four or five patches (Fig. 2, D to F) were similar to those obtained with whole oocyte voltage clamping, with faster decay rates for M4 currents than for type III or M5 currents. The times to achieve 50% decay were 7.5, 26.9, and 33.1 ms for averaged M4, type III, and M5 currents.

All channel types had a high proportion of very short openings, with durations near the limits of resolution of the recording system. The duration of bursts of openings was not limited in this way and was analyzed with a critical cut-off closed time to mark the beginnings and ends of bursts (12). A probability distribution of burst durations of the three kinds of Na⁺ channels is shown in Fig. 3A. Each patch contained one to three channels. At a test potential of 0 mV, the mean burst duration in M4 and M5 channels was significantly shorter than type III (3.17 and 2.27 ms versus 11.4 ms, $P < 0.02$, Kolmogorov-Smirnov two-sample test). At least two sets of oocytes were injected on separate occasions in each case. Because M5 channels showed briefer bursts but a similar rate of macroscopic current decay to type III channels, we compared probability distributions of latencies to first opening, or waiting times (Fig. 3B). The distributions for type III and single-channel M4 currents were not significantly different (Kolmogorov-Smirnov two-sample test), whereas the waiting time of M5 currents was significantly prolonged ($P < 0.001$, Kolmogorov-Smirnov two-sample test). The waiting time to first opening as a function of test potential in a patch containing a single Na⁺ channel expressed from M5 mRNA is shown in Fig. 3C. Stronger depolarizations caused shorter waiting times and fewer null traces, but activation gating was slower than type III or M4 channels at all potentials.

The kinetics of the single-channel currents are consistent with presently favored models in which Na⁺ channels enter a long-lived inactivated state in a mainly voltage-independent manner, and activation gating is strongly voltage-dependent (13, 14). The briefer burst durations of M4 and M5 currents are consistent with faster entry into the inactivated state. Activation gating, however, was notably slower for M5 currents. In this case, the two effects were offsetting and produced whole cell currents not significantly different from those of type III.

Type III Na⁺ channels inactivated slowly because of reopenings. Na⁺ channels from heart, skeletal muscle, and some types of nervous tissue also showed reopenings (14, 15). α -Scorpion toxin increased reopenings in both fast and slowly inactivating Na⁺ channels (16), suggesting a similar structural basis for both kinds of inactivation. We expected, therefore, that removal of positively charged elements of a pore-blocking ball should have the same effect on both kinds of inactivation and produce even slower inactivation of these type III Na⁺ channels. The peptide sequence linking regions III and IV was proposed as a likely candi-

date for the ball and chain of Na⁺ channel inactivation because the 11 lysines and 1 arginine might serve both as targets for endopeptidases, which remove inactivation, and as channel blockers, because of their positive charge. This model, in its simplest form, predicts that removing positive charges should delay inactivation gating without affecting activation gating. In our experiments the results were the opposite. Moreover, the III-IV linker is not restricted in its effects to inactivation; removal of one positive charge slowed activation. This finding supports the concept of a cytoplasmic element that is involved in both activation and inactivation gating and is consistent with other findings in K⁺ channels (17, 18). Hence the III-IV linker has more complex effects on Na⁺ channel gating than previously postulated.

Sodium channel gating is sensitive to the presence of positive charges between residues 1426–1461 in the III-IV linker. Lysines 1426–1428 may be crucial to normal channel function, as the mutation of all three to asparagines yielded no functional channels. We speculate that removal of positive charges alters the electrostatic interactions of the linker with other parts of the channel protein (19), particularly the nearby positively charged S4 segments and the conserved negative charges in the COOH-terminus of the channel protein. Alternatively, the III-IV linker might serve as the binding site for another blocking area of the molecule, in which case the negatively charged glutamate residues at positions 1438 and 1439 might be pivotal in inactivation gating.

REFERENCES AND NOTES

1. M. Noda *et al.*, *Nature* **320**, 188 (1986).
2. H. R. Guy and P. Seetharamulu, *Proc. Natl. Acad. Sci. U.S.A.* **83**, 508 (1986).
3. R. E. Greenblatt, Y. Blatt, M. Montal, *FEBS Lett.* **193**, 125 (1985).
4. P. M. Vassilev, T. Scheuer, W. A. Catterall, *Science* **241**, 1658 (1988); *Proc. Natl. Acad. Sci. U.S.A.* **86**, 8147 (1989).
5. W. Stühmer *et al.*, *Nature* **339**, 597 (1989).
6. C. M. Armstrong, F. Bezanilla, E. Rojas, *J. Gen. Physiol.* **62**, 375 (1973); C. M. Armstrong and F. Bezanilla, *ibid.* **70**, 567 (1977).
7. R. W. Aldrich, *Nature* **339**, 578 (1989).
8. For preparation of mutants, a 1.9-kb Hind III fragment [positions 3498 to 5438; R. H. Joho *et al.*, *Mol. Brain Res.* **7**, 105 (1990)] was subcloned into M13mp19. Site-directed mutagenesis was performed with the Amersham kit. Synthetic oligonucleotides with the appropriate base changes (up to three mismatches) plus ten complementary nucleotides on either side were used. An 815-bp Hpa I–Nar I fragment carrying the mutations was isolated from the mutated Hind III fragment and cloned back into the Na⁺ channel type III DNA between the Hpa I site (position 4096) and the Nar I site (4910). The DNA sequence between the Hpa I and the Nar I sites of the mutants was ascertained by sequencing the double-stranded full-length type III constructs. Cloning and subcloning of full-length Na⁺ channel complementary DNAs were made difficult by the frequent appearance of deletions

when the molecule was reassembled. This limited the number of mutations that could be tested. Methods for oocyte harvesting, RNA injection, whole cell and single-channel recording have been reported [R. H. Joho *et al.*, above; J. R. Moorman *et al.*, *Am. J. Physiol.* **253**, H985 (1987)]. Single channel current traces were idealized with a program written by A. M. J. Van Dongen and implemented by H. Nguyen. The algorithm uses a dI/dt threshold for determining transitions between open and closed states. The idealized traces were used to construct frequency histograms of closed times, burst durations, and waiting times to first opening. The data were represented by a single or sum of two exponentials model where the parameters were estimated with a maximum likelihood technique. Cumulative distributions of waiting time to first opening were corrected for the number of channels in the patch.

9. J. R. Moorman, G. E. Kirsch, A. M. Brown, R. H. Joho, unpublished observations.

10. C. Methfessel *et al.*, *Pfluegers Arch.* **407**, 577 (1986).

11. J. R. Moorman, G. E. Kirsch, A. M. J. Van Dongen, R. H. Joho, A. M. Brown, *Neuron* **4**, 243 (1990).

12. D. Colquhoun and B. Sakmann, *J. Physiol. (London)* **369**, 501 (1985).

13. R. W. Aldrich, D. P. Corey, C. F. Stevens, *Nature* **306**, 436 (1983); R. W. Aldrich and C. F. Stevens, *J. Neurosci.* **7**, 418 (1987).

14. G. E. Kirsch and A. M. Brown, *J. Gen. Physiol.* **93**, 85 (1989).

15. D. L. Kunze, A. E. Lacerda, D. Wilson, A. M. Brown, *ibid.* **86**, 691 (1985); J. B. Patlak and M. Ortiz, *ibid.* **87**, 305 (1986); B. A. Barres, L. L. Y. Chun, D. P. Corey, *Neuron* **2**, 1375 (1989).

16. G. E. Kirsch, A. Skattebol, L. D. Possani, A. M. Brown, *J. Gen. Physiol.* **93**, 67 (1989).

17. L. C. Timpe, Y. N. Jan, L. Y. Jan, *Neuron* **1**, 659 (1988).

18. W. Stühmer *et al.*, *EMBO J.* **8**, 3235 (1989); A. M. J. Van Dongen, G. C. Frech, J. A. Drewe, R. H. Joho, A. M. Brown, *Neuron*, in press.

19. In these electrostatic models we assume that the charged regions lie within a Debye length of one another in the cytoplasm or that they lie within hydrophobic regions of low dielectric constant. A nonelectrostatic explanation may also apply in which removal of lysines or the arginine changes the sensitivity of the mutant channels to endogenous proteases, which in turn leads to altered channel gating.

20. We thank H. Silberberg for preparation of the mutant mRNAs, K. Kasper for DNA sequencing, and G. Schuster for oocyte injection. Supported by research grants KL-01858 (J.R.M.), HL-36930 and NS-23877 (A.M.B.) from the NIH, the Advanced Technology Program of the State of Texas (R.H.J.) the Kempner Foundation and the Sealy Memorial Endowment (J.R.M.), and the American Heart Association, Texas affiliate (R.H.J. and G.E.K.).

12 April 1990; accepted 17 July 1990

Behavioral Effects of Progesterone Associated with Rapid Modulation of Oxytocin Receptors

MICHAEL SCHUMACHER,* HÉCTOR COIRINI, DONALD W. PFAFF, BRUCE S. McEWEN

The ventromedial nuclei of the hypothalamus (VMN) are important for the control of feminine mating behavior, and hormone action within these nuclei has been causally related to behavior. Estradiol induces receptors for oxytocin in the VMN and in the area lateral to these nuclei over the course of 1 to 2 days, and progesterone causes, within 30 minutes of its application, a further increase in receptor binding and an expansion of the area covered by these receptors lateral to the VMN. The rapid progesterone effect appears to be a direct and specific effect of this steroid on the receptor or membrane, because it was produced *in vitro* as well as *in vivo* and was not mimicked by a variety of other steroids. The effect of progesterone occurred in the posterior part of the VMN, where oxytocin infusion facilitated feminine mating behavior; it did not take place in the anterior part of the VMN, where oxytocin infusion had no effect on mating behavior.

IT IS GENERALLY ACCEPTED THAT STEROID hormones can regulate cellular functions in the brain and certain behaviors by modulating gene expression after binding to intracellular receptors (1, 2). Steroid hormones also rapidly affect the excitability of brain cells *in vitro* or when applied electrophoretically by changing ion conductances, the release of neurotransmitters, or the char-

acteristics of neurotransmitter receptors (3). These rapid hormone effects can be observed in brain regions such as the cerebellum and the cortex that contain no measurable intracellular steroid receptors (4). The physiological significance of these observations remains uncertain (5) because no rapid membrane effects of steroids have been causally related to the activation of a behavioral response. We now show the modulation of estrogen (E)-induced oxytocin receptors by progesterone (P), a rapid steroid effect that appears to be involved in the facilitation of a complex behavior, feminine mating (lordosis) behavior in the rat (6).

Progesterone induces an expansion of the area covered by oxytocin receptors in the

ventromedial hypothalamus of female rats primed with E (7). This spread of oxytocin binding occupies the area lateral to the VMN, which contains oxytocin-immunoreactive fibers and the long dendrites and axons of VMN neurons (7, 8). Oxytocin infused into the area lateral to the VMN facilitates lordosis behavior only in female rats primed sequentially with E and P and not in females treated with E alone (7). This behavioral effect can be blocked by a specific antagonist of oxytocin (9). We have examined this modulation of oxytocin receptor binding by P and its relation to lordosis behavior.

Oxytocin receptor binding to brain sections was quantified by *in vitro* receptor autoradiography (10). Iodinated [$d(\text{CH}_2)_5$, Tyr(Me)², Thr⁴, Tyr-NH₂⁹] ornithine vasotocin analog ([¹²⁵I]OVTA) was used as a ligand for the central oxytocin receptor because of its high specificity, affinity (K_D , 50 pM), and specific activity (2200 Ci/mmol) (11). Initially, we examined the regional distribution of oxytocin receptor binding within the ventromedial hypothalamus and changes in this binding induced by P in ovariectomized (OVX) and adrenalectomized (ADX) female rats primed with estradiol benzoate (EB). Brains of EB-primed females were sampled for oxytocin receptor autoradiography at different times after the injection of vehicle (EB only) or P (EB + P) (12). In the anterior part of the ventromedial hypothalamus, oxytocin receptor binding was limited to the cell body region of the VMN and was not affected by P treatment (Figs. 1 and 2). In the posterior ventromedial hypothalamus of EB-primed females, oxytocin receptor binding occurred in the ventrolateral parts of the VMN but also extended into the area lateral to the nuclei (Fig. 1). In the posterior VMN, P treatment only slightly increased the oxytocin receptor binding in the cell body region (5 to 8%), but it increased oxytocin receptor binding by more than 25% in the surrounding neuropil (Figs. 1 and 2). This increase in binding density was accompanied by an expansion of the area covered by oxytocin receptors. This effect of P could be observed within 30 min and it lasted for at least 8 hours (Fig. 2).

Because P increases the synthesis of new proteins in the VMN (2, 13), we determined whether the increase in oxytocin receptor binding produced by P involves the rapid synthesis of new receptors (14). We tried to block the effects of P with the protein synthesis inhibitor anisomycin. Fifteen minutes before injecting 0.5 mg of P or vehicle, EB-primed females were injected with saline or with 100 mg of anisomycin per kilogram of body weight in saline (15). This amount of anisomycin inhibits cerebral protein syn-

M. Schumacher, H. Coirini, B. S. McEwen, Laboratory of Neuroendocrinology, The Rockefeller University, 1230 York Avenue, New York, NY 10021.
D. W. Pfaff, Laboratory of Neurobiology and Behavior, The Rockefeller University, 1230 York Avenue, New York, NY 10021.

*To whom correspondence should be addressed.